TOPTICA Clock Laser System

Dr. Florian Schäfer, Dewni Pathegama, Dr. Filippo Bregolin
TOPTICA Photonics SE

This white paper presents the design, implementation, and performance evaluation of the TOPTICA Clock Laser System, CLS, a commercial ultra-stable laser system optimized for precision quantum applications such as optical clocks, quantum simulation and quantum computers. The system consists of an external cavity diode laser which is frequency stabilized to a high-finesse optical cavity. This generates laser light with a fractional frequency instability below 2×10^{-15} at 1 s averaging time, providing high frequency stability to drive the very narrow atomic transitions required for these applications and to serve as a high-quality optical local oscillator. In this paper, the frequency stability of the system is investigated, possible sources of noise and their impact on the system stability are discussed, and the implemented mitigation strategies are presented. Then, using a cross-correlation approach, the final system frequency noise performance is assessed, and the applicability of commonly used linewidth definitions is discussed.

1 INTRODUCTION

Ultra-stable optical local oscillators are at the heart of many atomic experiments and applications such as optical clocks [1], quantum simulators [2], and quantum computers [3, 4], where exceptional frequency and phase stability are required to drive narrow atomic transitions and to keep a precise phase reference. With the increasing interest in bringing these technologies into academic and commercial applications, both inside and outside of laboratories, compact laser systems with robust design and minimal operational oversight are becoming an industrial demand.

The TOPTICA Clock Laser System is designed to fulfill the requirements of such optical local oscillators and is available in tabletop (CLS) and fully 19”-rack mounted (MCLS) versions. The (M)CLS is available for a wide range of wavelengths from visible to infrared to address clock transitions in neutral atoms like Yb, Sr, Th, ions like Yb^+, Sr^+, Ca^+, Ba^+, and, in addition, to be employed as a stable reference for optical frequency combs.

This white paper is organized as follows: Section 2 reviews the basics of ultra-stable lasers. In Sec. 3 the impact of various environmental noise sources on the laser stability, the implemented mitigation strategies, and experimental CLS performance data on their effectiveness are presented. Section 4 discusses strategies to quantify the stability of ultra-stable lasers in general and presents the corresponding results of a TOPTICA clock laser system in particular. A general discussion of the concept of laser linewidth, its applicability to ultra-stable lasers and some exemplary evaluations follows in Sec. 5. Finally, Sec. 6 summarizes the findings and concludes the presented work.

2 REALISING AN ULTRA-STABLE LASER

At the center of an ultra-stable laser system lies a stable frequency reference. A source laser is stabilized to that reference, thereby transferring the stability of the reference to the laser frequency. In the CLS the frequency reference is a high-finesse (about 200,000) optical cavity in a Fabry-Pérot design. To achieve this ele-

vated finesse, the mirror reflectivity must be higher than 99.9985 %. Note that for infrared CLS systems, the finesse is generally even higher than for visible systems due to lower scattering and absorption losses on the cavity mirrors. Once a stable frequency reference is available, the laser frequency is stabilized to an optical resonance of this reference using a feedback control loop based on the Pound-Drever-Hall technique [5]. Fast noise control electronics allow for a proper transfer of the short-term stability of the frequency reference to the source laser frequency. Specialized, slower control electronics keep the transfer long-term stable and faithful to the reference.

As the resonance frequency of an optical cavity varies with its optical path length (and therefore its geometrical length), environmental disturbances that affect the cavity length will influence the CLS performance. For example, to achieve a relative laser instability at the 10^{-15} level by referencing it to an optical cavity with a mirror spacing of 10 cm, the absolute length stability of the cavity has to be on the 0.1 fm level. For comparison, the proton diameter is at 1.7 fm more than ten times larger than this length stability requirement. It is therefore of paramount importance to implement strategies to keep the optical path length inside the cavity, and therefore the resonance frequency, as stable as possible.

The CLS cavity consists of an ultra-low expansion (ULE®) glass spacer 10 cm in length and two mirrors optically contacted to either side of it, with a resulting free spectral range of 1.5 GHz. The mirrors are made of a fused silica (FS) substrate and coated with a highly reflective dielectric coating. The cavity design, including the FS mirrors, allows for a thermal-noise-limited fractional frequency instability below 4×10^{-16} in terms of Allan deviation. At a still compact footprint, the cavity length ensures smaller cavity resonance linewidths (7.5 kHz for a finesse of 200,000) than shorter, e.g. 5 cm, designs might provide.

ULE® glass offers the advantage that the temperature at which its coefficient of thermal expansion (CTE) reaches zero is close to room temperature (i.e., between 20 °C and 35 °C). At this temperature, the cavity length is insensitive to small temperature changes. To compensate for the CTE mismatch between the ULE® spacer and FS mirror substrates, additionally two ULE® rings are optically contacted to the outer facets of the two mirrors [6]. The zero-crossing CTE temperature is measured and preset as the operating temperature of the cavity via an active temperature stabilization control loop (discussed further in Sec. 3.2).

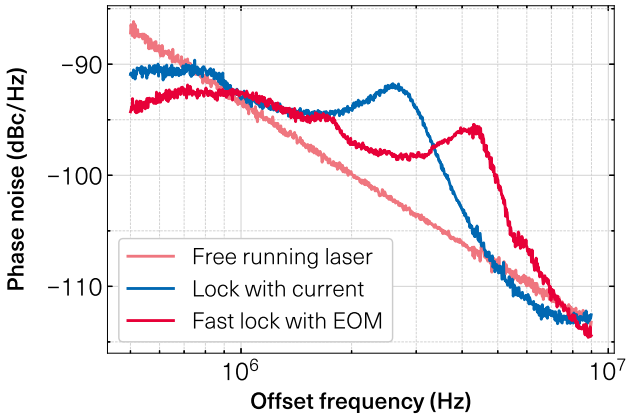

Fig. 1: Laser phase noise power spectral density. The increase in locking bandwidth when locking feedback is provided to an ECDL intra-cavity EOM (dark red trace) as compared to the diode current (blue trace) is visible in a shift of the loop-resonance peak position. Also shown is the phase noise of the free running ECDL (light red data).

The source laser is a TOPTICA external cavity diode laser (ECDL), whose frequency can be modulated by varying the laser diode current. Alternatively, if the ECDL is provided with an intra-cavity EOM (available as “F” option), the frequency can be modulated by varying the EOM voltage, enabling a larger modulation bandwidth of up to 4.5 MHz, as opposed to about 2.5 MHz with current control, see Fig. 1. In both cases, the laser frequency can additionally be modulated by varying the laser external cavity length via a piezo actuator. This control loop has a lower control bandwidth but a much larger dynamic range, which enables the source laser to stay in lock over several weeks[1].

3 MITIGATION OF ENVIRONMENTAL NOISE

This section details the most common sources of noise that affect the stability of cavity-referenced lasers, what strategies are implemented to limit their impact on the

[1] The time during which the source laser stays in lock depends on the mode stability of the source laser.

CLS, and exemplary performance data of the effectiveness of those measures. In all cases the system stabilities are estimated by comparing the CLS against an independent reference laser system with similar or better performance. See Sec. 4 for an in-depth analysis of the final CLS performance. Note that in the present paper all Allan deviation data is calculated and shown after having removed any linear frequency drifts from the data (which in actual applications can be implemented by suitable dedrifting strategies, see Sec. 3.7).

3.1 AIR PRESSURE FLUCTUATIONS

The cavity optical path length depends on the index of refraction of the medium between the mirrors. This medium is air, whose index of refraction is pressure dependent. Accordingly, there is a direct correlation between any air pressure fluctuations and the stability of the cavity frequency. One finds, that the relative change of the index of refraction of air depends on the absolute air pressure [7] with a conversion factor of roughly 2.6×10^{-7} mbar^{-1}. Therefore, to limit the instabilities of the laser frequency due to air pressure fluctuations to the 10^{-16} level, it is necessary to keep the air pressure stable to about 4×10^{-10} mbar. To shield the cavity from environmental pressure fluctuations within the required levels, it is housed inside a vacuum chamber, which, by means of an active ion pump, maintains a constant low pressure of typically below 5×10^{-8} mbar. In consequence, the relative air pressure inside the vacuum chamber only needs to be stable on the percent level to not limit the laser stability. Holding the cavity in a vacuum also prevents thermal conductivity by convection and thus strongly isolates the cavity from environmental temperature fluctuations.

3.2 TEMPERATURE VARIATIONS

The effect of environmental temperature fluctuations is, in addition to the vacuum chamber external housing, further suppressed by locating the cavity inside two in-vacuum aluminum thermal shields (shown in Fig. 2, a). The vacuum chamber itself is wrapped in a thermally insulating foil and, together with the optical components required for frequency stabilization, is installed within an aluminum housing. This custom-engineered aluminum housing (shown in Fig. 2, b) provides a mechanically solid environment, which also serves as an additional thermal radiation shield. One of the inner thermal shields and the vacuum chamber itself are actively temperature controlled, using two pairs of Peltier elements, which ensures temperature stabilization at the 0.1 mK (measured in-loop) level. The overall suppression of external temperature perturbations has been experimentally assessed for environmental 2.0 °C peak-to-peak temperature oscillations with 6-hour period, which led to 0.001 °C temperature changes at the innermost, passive thermal shield (Fig. 3). The cavity itself will then experience even smaller temperature variations. This confirms for this timescale a suppressed impact of external temperature perturbations on the frequency noise power spectral density (PSD) in excess of 64 dB. Note

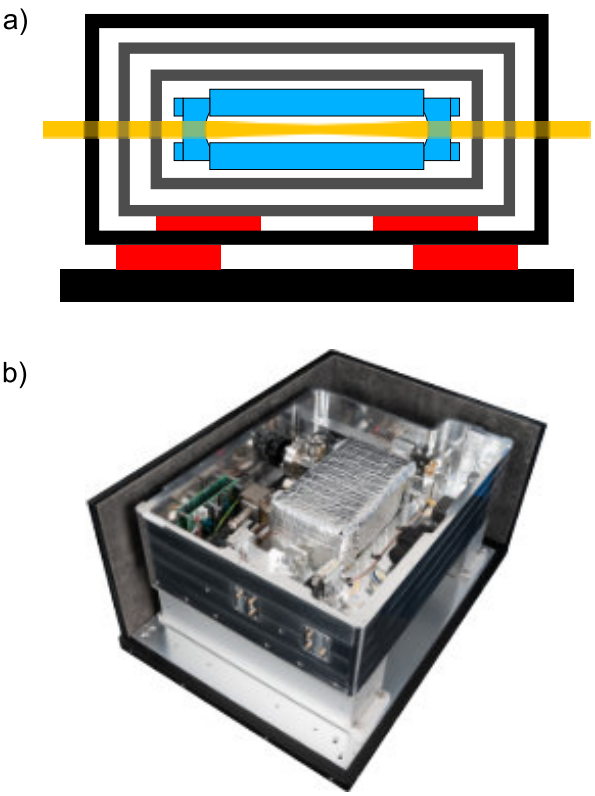

Fig. 2: Basic CLS layout. a) The high-finesse cavity (blue) is embedded in a vacuum chamber (black) and several thermal shields (gray). Active temperature stabilization is via Peltier elements (red). b) The cavity and the required optics are located in a solid aluminum housing, which is resting on top of an active vibration isolation solution and inside an outer acoustic enclosure (having partially been opened in the present picture).

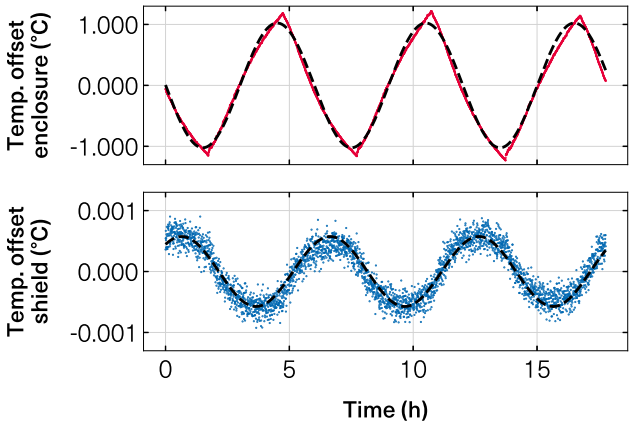

Fig. 3: Response of the CLS to environmental temperature variations. Upper panel: Forced temperature offsets induced to the CLS acoustic enclosure (red data). Lower panel: Residual temperature offset modulation at the innermost, passive shield of the cavity assembly (blue data). Both data sets are approximated by sine curves with periods of 6 hours (dashed lines).

that such slow variations, typical for day-night temperature cycles, pose the greatest temperature stabilization challenges due to the intrinsic low-pass filtering behavior of the passive temperature isolation shields.

The cavity spacer geometry and the mechanical mounting of the cavity inside the vacuum chamber are both optimized to passively minimize the effect of environmental temperature fluctuations and seismic vibrations on the cavity length, while still allowing the cavity to be transported under vacuum. The initial design for both components was developed and patented by the Physikalisch Technische Bundesanstalt (PTB), the national metrology institute of Germany, and is licensed to TOPTICA.

3.3 RESIDUAL AMPLITUDE MODULATION

The electro-optic modulator (EOM) used to implement the Pound-Drever-Hall method of frequency stabilization introduces some parasitic and undesired amplitude modulation along with the phase modulation. This is referred to as residual amplitude modulation (RAM) and is an unavoidable byproduct of phase modulation based on the electro-optic effect [8]. Additionally, RAM can be generated by other effects, such as time-varying etalons, i.e., reflections between parallel surfaces along the beam path to the cavity. This amplitude modulation can lead to a time-dependent offset of the error signal used for the frequency stabilization loop and thereby add a shift to the laser frequency compared to the actual cavity resonance. In the CLS, spurious etalons are suppressed via an optical isolator. Additionally, the opto-mechanical design ensures that all optical components have predefined positions that avoid parallel surfaces in a reproducible way. EOM-induced RAM is passively constrained by construction, using a crystal with a wedged surface, which geometrically separates the ordinary and extraordinary beams propagating in the EOM [9]. By active variation of the EOM temperature [10] the residual fractional frequency offset induced by RAM is estimated to be below 5×10^{-16} for temperature changes of the EOM below 0.1 °C.

3.4 SEISMIC AND ACOUSTIC NOISE

The aluminum housing containing the vacuum chamber and the optical components is placed on top of a vibration isolation table to actively decouple the system from environmental vibrations (see Fig. 2, b). This reduces the seismic noise at the cavity by up to 30 dB, leading even in vibrationally quiet basement laboratories to improved stabilities by up to an order of magnitude (see Fig. 4). Finally, the system is fully enclosed by an acoustic enclosure, which passively shields the system from acoustic noise, temperature fluctuations, and general air-flow effects. The acoustic noise suppression achieved by the acoustic enclosure has been measured to be around 20 dB in the frequency range 100 Hz to 1 kHz and approx. 30 dB up to 20 kHz.

Optionally, in challenging environments a low-frequency seismic sensor (Seismic+ option) can be used in addition to the active vibration isolation table to further improve the seismic isolation in the low-frequency range, down to 0.2 Hz. The data of Fig. 5 shows the measured seismic noise spectrum on the third floor of a standard office building. There, vibrations are easily one order of magnitude larger than in an optical-grade basement laboratory. While the standard vibration isolation table dramatically reduces seismic noise, the additional Seismic+ solution brings the noise level nearly on par with standard vibration isolated basement laboratory levels.

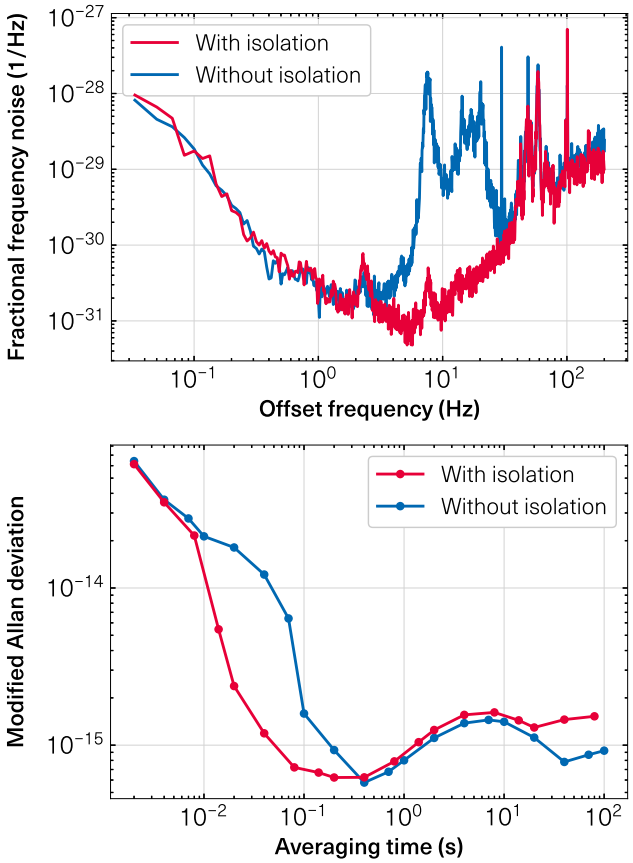

Fig. 4: Stability of a CLS with (red) and without (blue) seismic and acoustic isolation. Top panel: Fractional frequency noise in terms of power spectral density. Bottom panel: Fractional frequency instability evaluated via the modified Allan deviation.

3.5 OPTICAL POWER FLUCTUATIONS

Once the cavity is isolated properly from external environmental factors, the fundamental limit to its length stability is posed by thermal noise. A fraction of the optical power entering the cavity is absorbed by the cavity components. If the optical power fluctuates, this will lead to variations in the absorbed power, leading to fluctuations in the temperature of the cavity components. These temperature variations will cause optical path length changes inside the cavity via expansion and contraction of the cavity mirror coatings and changes in the refractive index of the mirror substrates. Therefore, it is important to stabilize the optical power circulating inside the cavity. Typically, for a frequency stability of about 0.1 Hz it is necessary to keep the optical power before the cavity stable on the nano-Watt level. In the

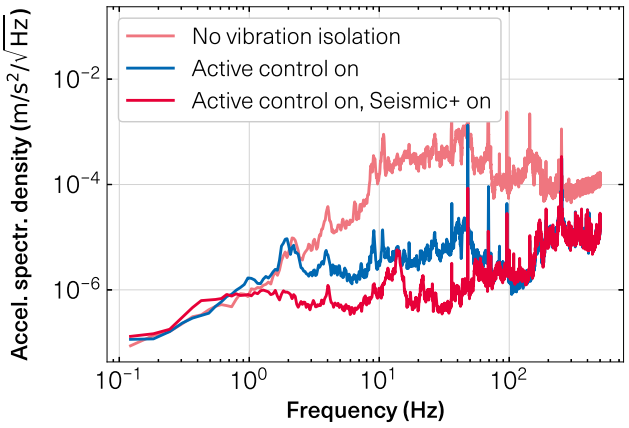

Fig. 5: Performance of the default CLS active vibration isolation and Seismic+ option in terms of acceleration power spectral density recorded on the third floor of an office building.

CLS, the optical power is stabilized by acting on the efficiency of either an acousto-optic modulator (AOM) or an electro-optic modulator (EOM) with a residual rms power fluctuation of below 5 nW over 3 hours of measurement time. For an optical cavity at 729 nm with a finesse of about 200,000, this corresponds to a residual rms fractional frequency noise of below 3×10^{-16} or, in terms of Allan deviation, an instability of better then 9×10^{-17} for averaging times longer than 1 s. The importance of actively stabilizing the power inside the cavity is demonstrated in Fig. 6, where the onset of a degradation of the frequency stability without power stabilization is in the Allan deviation already visible for averaging times starting from 0.1 s.

3.6 FIBER NOISE CANCELLATION

When the laser frequency is stabilized to the cavity resonance and a stable laser frequency is achieved, this laser light has to be delivered through an optical fiber to an application that could be a few meters away in the same laboratory or a few hundred meters away in a different building. While traveling through an optical fiber, the laser light inevitably acquires some phase noise caused by various environmental perturbations acting on the optical fiber along the optical path. This phase noise degrades the frequency stability of the laser beam arriving at the application, especially at offset frequencies up to about 1 kHz. To ensure that the

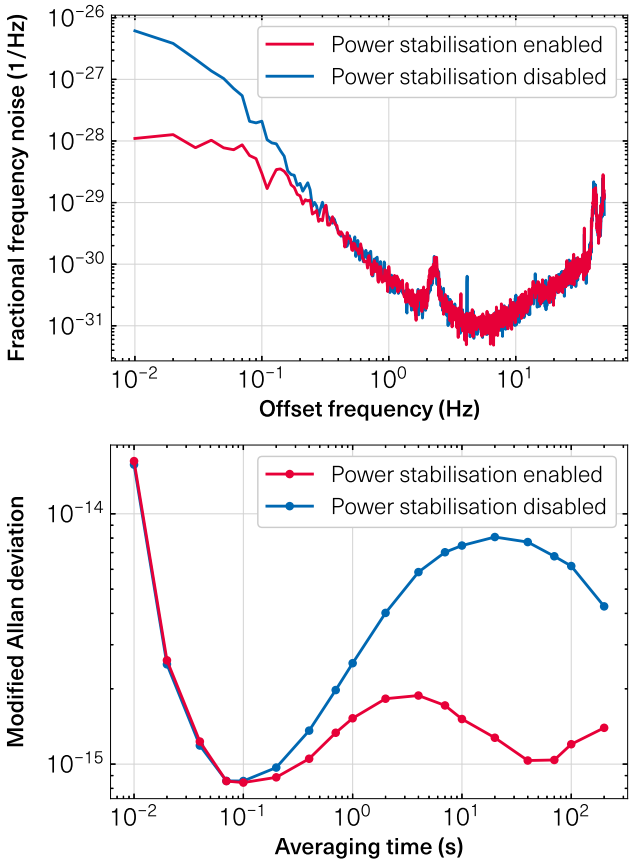

Fig. 6: Stability of a CLS with (red) and without (blue) optical power stabilization in front of the cavity. The organization of the Figure is as before.

CLS performance is not affected by the fiber delivery, a fiber noise cancellation (FNC) scheme [11] is used as an Add-On to the CLS to provide real-time compensation of the phase noise introduced by the fiber. The scheme is based on an adapted Michelson interferometer, where the phase noise acquired by the light as it travels through the optical fiber is measured as an optical beat signal on a fast photodiode and actively compensated via a phase-locked loop acting on an AOM. For a 20 m long polarization-maintaining fiber, the in-loop noise of the FNC phase-locked loop normalized to the laser frequency is measured to be well below 1×10^{-17} at 1 s integration time (in terms of modified Allan deviation), see Fig. 7. The effect on the light after the fiber is detailed in Fig. 8, where, in case of missing FNC, both fast noise components due to vibrations of the fiber and slow variations due to temperature changes can be distinguished.

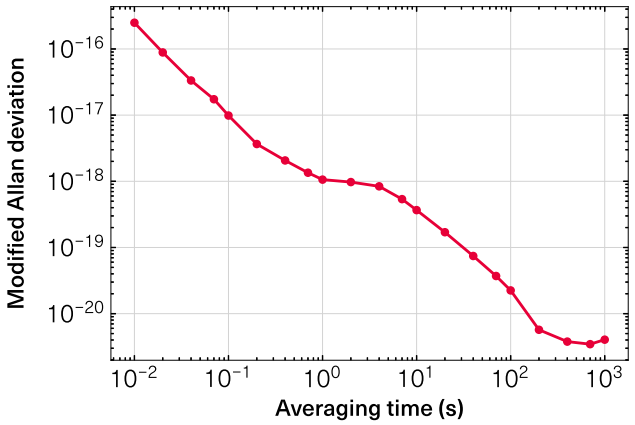

Fig. 7: In-loop noise of the CLS FNC phase-locked loop. Shown is the modified Allan deviation of the FNC interferometer photodiode signal, normalized to the CLS laser frequency.

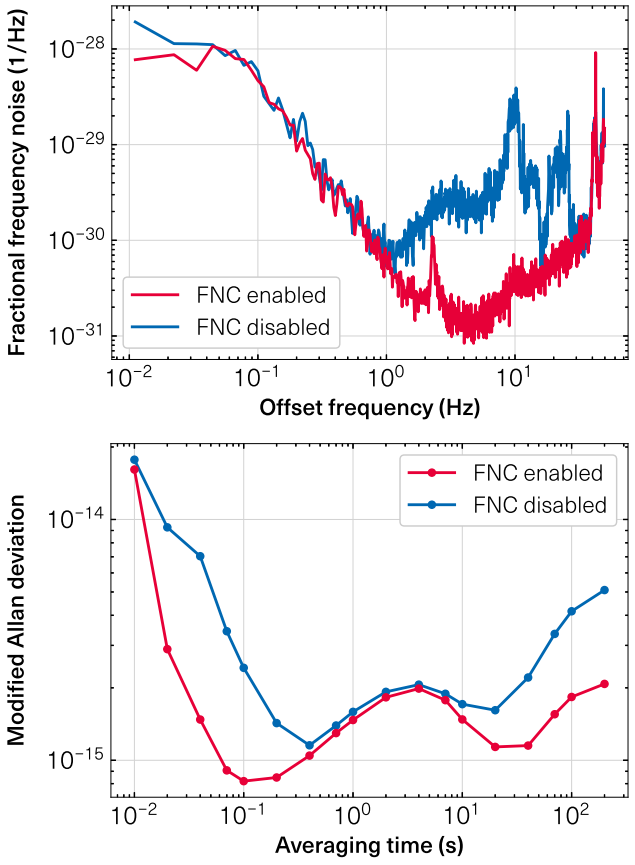

Fig. 8: Stability of CLS light after a 20 m fiber with (red) and without (blue) active fiber noise cancellation (FNC). The organization of the panels is as before.

3.7 FREQUENCY BRIDGE

With the laser locked to a resonance of the cavity, the laser frequency lies exactly at the frequency of the cavity mode it is locked to and cannot be further tuned. To allow flexible tuning of the cavity-stabilized laser frequency, a frequency bridge can be included in the CLS (CLS Bridge Add-On). This allows the laser frequency to be tuned to a specific frequency, e.g., a specific transition frequency in atomic spectroscopy. Additionally, the CLS Bridge can be used to compensate for the inevitable linear drift of the cavity (which for the TOPTICA CLS is typically well below 150 mHz/s already one year after initial deployment) by applying an opposite linear frequency ramp to the output frequency of the bridge. This Bridge Add-On can be realized using either a fiber-coupled broadband EOM with the sideband locking technique [12] or an AOM in a double-pass configuration [13]. In the case of the EOM, light traveling through an RF-driven EOM is phase modulated, generating optical sidebands. One of the sidebands is then locked to the cavity mode using the PDH technique. Once the laser is locked, by varying the frequency of the RF signal driving the EOM (varying the sideband frequency), the laser carrier frequency can be shifted with respect to the fixed cavity resonance. In the case of the AOM, light is sent twice through the AOM, which shifts the frequency of the light by twice the resonant frequency of the AOM before then being coupled to the cavity. By selecting an AOM with a suitable resonant frequency, the frequency of the light can be shifted to match the frequency required by the application.

4 SYSTEM STABILITY QUALIFICATION

Once a stable laser operation is established, its performance can be investigated by comparing it to a reference laser. However, this only gives access to relative stability information: unless the reference laser has significantly better stability than the laser under test, the measurement result will reflect the combined noise of both lasers. To assess the stability of only the device under test (DUT), usually at least two reference systems are needed. By comparing the three lasers against each other in a so-called “three-cornered hat” measurement, the extraction of the three individual stabilities in terms of the Allan deviations of each system is possible [14]. This approach, however, does not allow access to the frequency noise PSD of the DUT. Alternatively, a delayed self-heterodyne (DSHD) measurement can be performed to measure the DUT frequency noise PSD [15]. There, the sensitivity of the DSHD method depends on the length of the delay fiber used. The longer the fiber, the more sensitive the method. However, longer delay fibers also lead to more frequent poles in the frequency analysis. As a tradeoff, in the present work a delay fiber of 6 m length is used. This here results in a noise floor of the fractional frequency noise PSD of approx. $9 \times 10^{-28}\,\mathrm{Hz}^{-1}$ and allows one to assess the frequency noise of the DUT for frequencies above roughly 500 kHz. To overcome the limitations of both methods, a cross-correlation analysis can be utilized [16]. In this approach, two beat signals are generated by mixing the DUT with two reference laser systems, and the data is collected using a fast-sampling oscilloscope and a frequency counter. In short, each beat signal contains correlated data (the phase noise of the DUT) and uncorrelated data (the phase noise of the reference systems). By conducting a cross-correlation analysis between the two measurements and averaging over multiple acquisitions, the uncorrelated noise is suppressed and the only correlated data, i.e., the phase noise PSD of the DUT, is maintained. Combining high-frequency data from the fast-sampling oscilloscope with long-term data from the frequency counter, this method allows for the determination of the stability of the CLS in terms of frequency noise PSD across a wide range of offset frequencies. The frequency stability in terms of the Allan deviation can, if required, be obtained by integration of the frequency noise PSD.

In the present work, with the sampling oscilloscope[2] a number of 10 time traces of 1 s duration at 50 MSa/s have been recorded, and 3600 s of data have been acquired with the frequency counter[3] at a gating time of 10 ms in frequency average mode. In the oscilloscope measurements all signals have been ensured to be well below 20 MHz to guarantee well-resolved beat signals with the chosen sampling rate. The results presented in Fig. 9 reveal a fractional frequency instability below 2×10^{-15} at 1 s averaging time. Additionally, the absolute phase noise PSD (in units of dBc/Hz) is given in

[2] Teledyne LeCroy HDO6054B
[3] K+K FXE phase and frequency counter

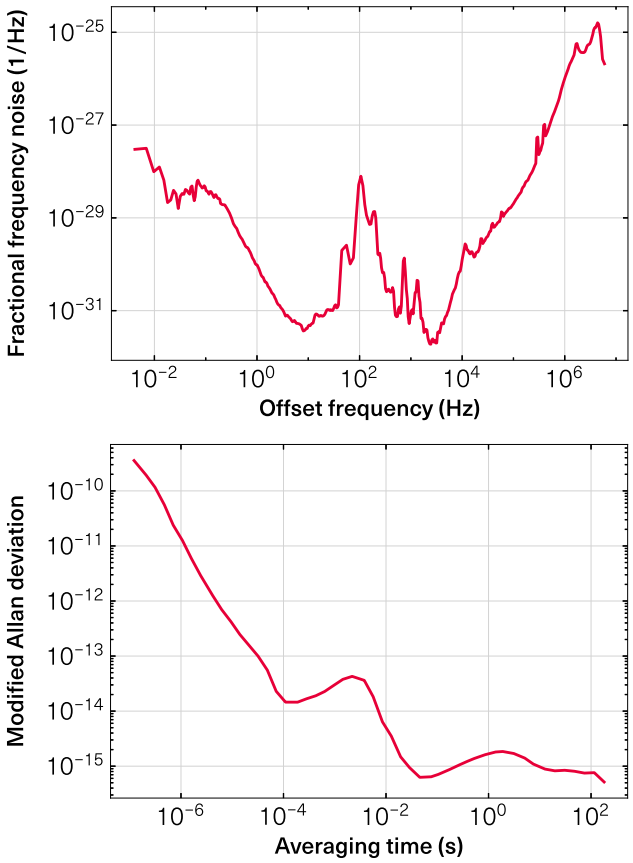

Fig. 9: Stability of a CLS operating at 729 nm, estimated via cross-correlation analysis using both a fast sampling oscilloscope and a frequency counter. The organization of the panels is as before.

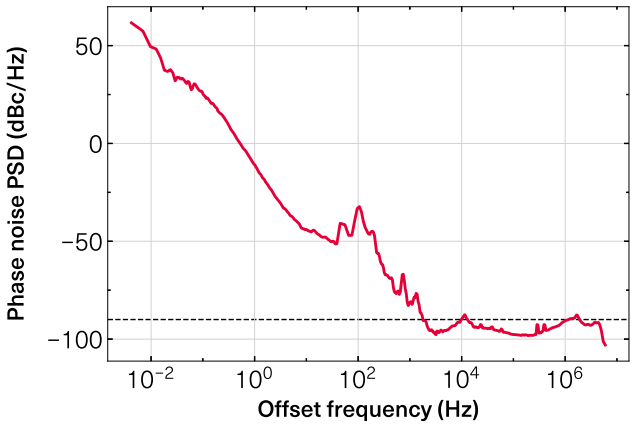

Fig. 10: Phase noise of a CLS at 729 nm. This is the same data as in the top panel of Fig. 9, but before normalization, and instead presented as a phase noise PSD in dBc/Hz. The dashed line indicates a phase noise level of -90 dBc/Hz.

Fig. 10. There, at high offset frequencies, a phase noise below around -90 dBc/Hz up to 4.5 MHz, corresponding to the PDH control bandwidth, is achieved.

In an independent set of control measurements (not reproduced here for brevity), the performance of the DUT has also been probed with a DSHD measurement and in a three-cornered-hat configuration. Both measurements are in excellent agreement with the high frequency range of the PSD data and for long averaging times in the Allan deviation, respectively.

The frequency noise PSD data reveals some increased noise in the vicinity of 100 Hz. This noise is mostly due to acoustic noise from a high-performance air filtration system in the same laboratory that has a prominent contribution from the included ventilation fans at around 100 Hz and which cannot be completely shielded from the cavity assembly by the acoustic enclosure (but which would be several orders of magnitude stronger without this enclosure). The next section will show that this increased noise does not limit the CLS performance in terms of common linewidth estimations.

5 CLS LINEWIDTH CONSIDERATIONS

A clock laser system is used in applications where the highest demands in terms of laser frequency and phase stability need to be fulfilled. The details of those requirements depend on the specific application. Optical atom clocks, quantum computers, quantum simulators, and high-precision sensors all have their specific phase stability profile needs. While for optical clock metrology long-term stability is of paramount importance, quantum computers often require the lowest possible phase noise in the few MHz offset frequency range. Therefore, the best available and most accurate source of information on the performance of a laser system and its suitability for a given target application is given by the frequency and/or phase noise PSD and the related Allan deviation.

It is, however, common practice to associate “traditional” lasers with a linewidth property [17], a convenient figure that summarizes a frequency spectrum with a single number. Depending on the expected linewidth of the laser, it might be measured with an optical spec-

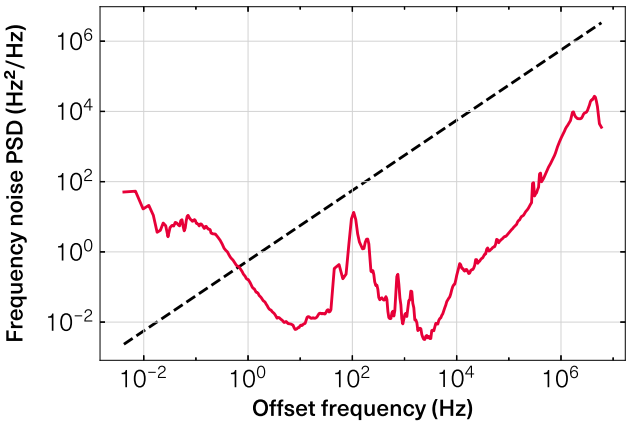

Fig. 11: Frequency noise of a CLS at 729 nm (red, solid) with indicated beta-separation line (black, dashed). In the beta-separation line approach, only those areas of the PSD at are above the beta-separation line contribute significantly to the laser linewidth.

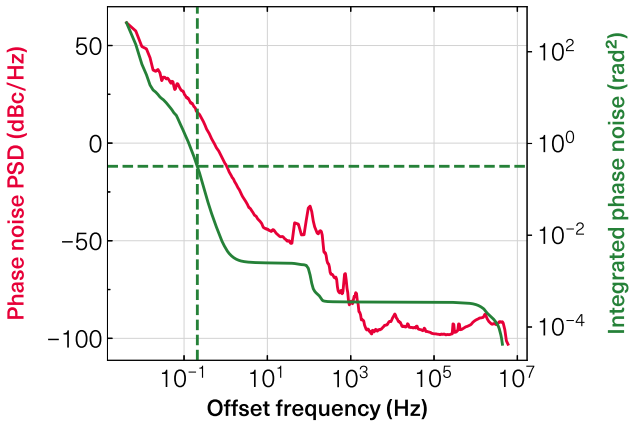

Fig. 12: Phase noise of a CLS at 729 nm (red, left axis) and corresponding integrated phase noise (green, right axis). The horizontal dashed line marks an integrated phase noise niveau of 1/π rad², the vertical dashed line indicates the frequency at which the CLS integrated phase noise drops below this level.

trum analyzer for very broad sources or by acquisition of the beat signal of two lasers with an RF spectrum analyzer. Both methods fail for very narrow (sub-Hz) lasers, such as ultra-stable clock lasers. There, even though the concepts of linewidth and lineshape themselves start to become ill-defined, mathematical linewidth calculation concepts might still be applied. In the following two common approaches, the beta-separation line method [18] and the 1/π rad² linewidth characterization [19], are applied to a TOPTICA CLS at 729 nm. Both approaches rely on integrations of certain areas of the frequency or phase noise PSD to derive characteristic quantities that either try to describe the line shape (beta-separation line) or the rms phase noise (1/π rad² linewidth) behavior.

In Fig. 11 the absolute frequency noise PSD of the system discussed in Sec. 4 is shown, now together with the corresponding beta-separation line. In the beta-separation line approach, only those parts of the frequency noise PSD that lie above the beta-separation line contribute to the major part of the linewidth shape. In the case at hand, the PSD data crosses the beta-separation line at 0.67 Hz. This implies that for integration times smaller than 1/(0.67 Hz) = 1.5 s this linewidth estimator becomes zero. Only for longer integration times is a non-zero result obtained. At 3 s the integral evaluates to 1.1 Hz, at 5 s it is 1.8 Hz, and at 10 s integration time a linewidth figure of 2.5 Hz is obtained. Note that the increased frequency noise around 100 Hz (see discussion in the previous section) is still well below the threshold defined by the beta-separation line and that in this sense does not significantly contribute to the system linewdith.

Similarly, Fig. 12 gives the phase noise PSD of the same system together with the integrated phase noise (where the integration runs over all frequencies larger than the chosen offset frequency). In the 1/π rad² linewidth approach, the linewidth is defined as the offset frequency where this integral equals 1/π rad², which here is at 0.2 Hz. This highlights the extreme phase stability of the CLS down to sub-Hz offset frequencies with respect to the central laser frequency.

6 CONCLUSIONS

In the TOPTICA clock laser system (M)CLS, an ECDL is frequency stabilized to a high-finesse optical cavity. To achieve reliable operation at the 10^{-15} instability level, a number of measures have been taken to guarantee the necessary isolation of the cavity from the relevant environmental fluctuations. A flexible bridge solution ensures long-term stable operation of the system at the correct laser frequency irrespective of the cav-

ity mode spectrum. Furthermore, an appropriate fiber noise cancellation scheme is introduced to also allow for transmission of the clock laser light via long optical fiber links to the application without loss of the excellent low-frequency and phase noise properties. The performance evaluations shown in the present work hold true for both the tabletop version of the system (CLS) and also for the fully rack-integrated variant (MCLS). This establishes the (M)CLS as a complete, stable, reliable, and easily field-deployable platform to serve as a high-quality optical local oscillator for advanced sensing, metrology, and quantum applications.

REFERENCES

[1] A. D. Ludlow, M. M. Boyd, J. Ye, E. Peik, and P. O. Schmidt: *Optical atomic clocks*, Rev. Mod. Phys. **87**, 637 (2015).

[2] I. M. Georgescu, S. Ashhab, and F. Nori: *Quantum simulation*, Rev. Mod. Phys. **86**, 153 (2014).

[3] L. Henriet, L. Beguin, A. Signoles, T. Lahaye, A. Browaeys, G.-O. Reymond, and C. Jurczak: *Quantum computing with neutral atoms*, Quantum **4**, 327 (2020).

[4] F. Bernardini, A. Chakraborty, and C. R. Ordóñez: *Quantum computing with trapped ions: a beginner's guide*, Eur. J. Phys. **45**, 013001 (2023).

[5] E. D. Black: *An introduction to Pound–Drever–Hall laser frequency stabilization*, Am. J. Phys. **69**, 79 (2001).

[6] T. Legero, T. Kessler, and U. Sterr: *Tuning the thermal expansion properties of optical reference cavities with fused silica mirrors*, J. Opt. Soc. Am. B **27**, 914 (2010).

[7] P. E. Ciddor: *Refractive index of air: new equations for the visible and near infrared*, Appl. Opt. **35**, 1566 (1996).

[8] E. A. Whittaker, M. Gehrtz, and G. C. Bjorklund: *Residual amplitude modulation in laser electro-optic phase modulation*, J. Opt. Soc. Am. B **2**, 1320 (1985).

[9] Z. Li, Y. Tian, Y. Wang, W. Ma, and Y. Zheng: *Residual amplitude modulation and its mitigation in wedged electro-optic modulator*, Opt. Express **27**, 7064 (2019).

[10] L. Li, F. Liu, C. Wang, and L. Chen: *Measurement and control of residual amplitude modulation in optical phase modulation*, Rev. Sci. Instrum. **83**, 043111 (2012).

[11] L.-S. Ma, P. Jungner, J. Ye, and J. L. Hall: *Delivering the same optical frequency at two places: accurate cancellation of phase noise introduced by an optical fiber or other time-varying path*, Opt. Lett. **19**, 1777 (1994).

[12] J. I. Thorpe, K. Numata, and J. Livas: *Laser frequency stabilization and control through offset sideband locking to optical cavities*, Opt. Express **16**, 15980 (2008).

[13] E. A. Donley, T. P. Heavner, F. Levi, M. O. Tataw, and S. R. Jefferts: *Double-pass acousto-optic modulator system*, Rev. Sci. Instrum. **76**, 063112 (2005).

[14] J. Gray and D. Allan: A Method for Estimating the Frequency Stability of an Individual Oscillator, in *28th Annual Symposium on Frequency Control* (IEEE, Atlantic City, NJ, USA, 1974), p. 243.

[15] T. Okoshi, K. Kikuchi, and A. Nakayama: *Novel method for high resolution measurement of laser output spectrum*, Electronics Lett. **16**, 630 (1980).

[16] E. Rubiola and V. Giordano: *Correlation-based phase noise measurements*, Rev. Sci. Instrum. **71**, 3085 (2000).

[17] S. Schmidt-Eberle: *Linewidth Measurement of Diode Lasers*, TOPTICA Photonics SE, 2023.

[18] G. D. Domenico, S. Schilt, and P. Thomann: *Simple approach to the relation between laser frequency noise and laser line shape*, Appl. Opt. **49**, 4801 (2010).

[19] D. Hjelme, A. Mickelson, and R. Beausoleil: *Semiconductor laser stabilization by external optical feedback*, IEEE Journal of Quantum Electronics **27**, 352 (1991).